Alzheimer's Therapeutics

DOI: 10.1002/ange.201104150

Inhibition of Beta-Amyloid Peptide Aggregation by Multifunctional Carbazole-Based Fluorophores**

Wanggui Yang, Yi Wong, Olivia T. W. Ng, Li-Ping Bai, Daniel W. J. Kwong, Ya Ke, Zhi-Hong Jiang, Hung-Wing Li, Ken K. L. Yung,* and Man Shing Wong**

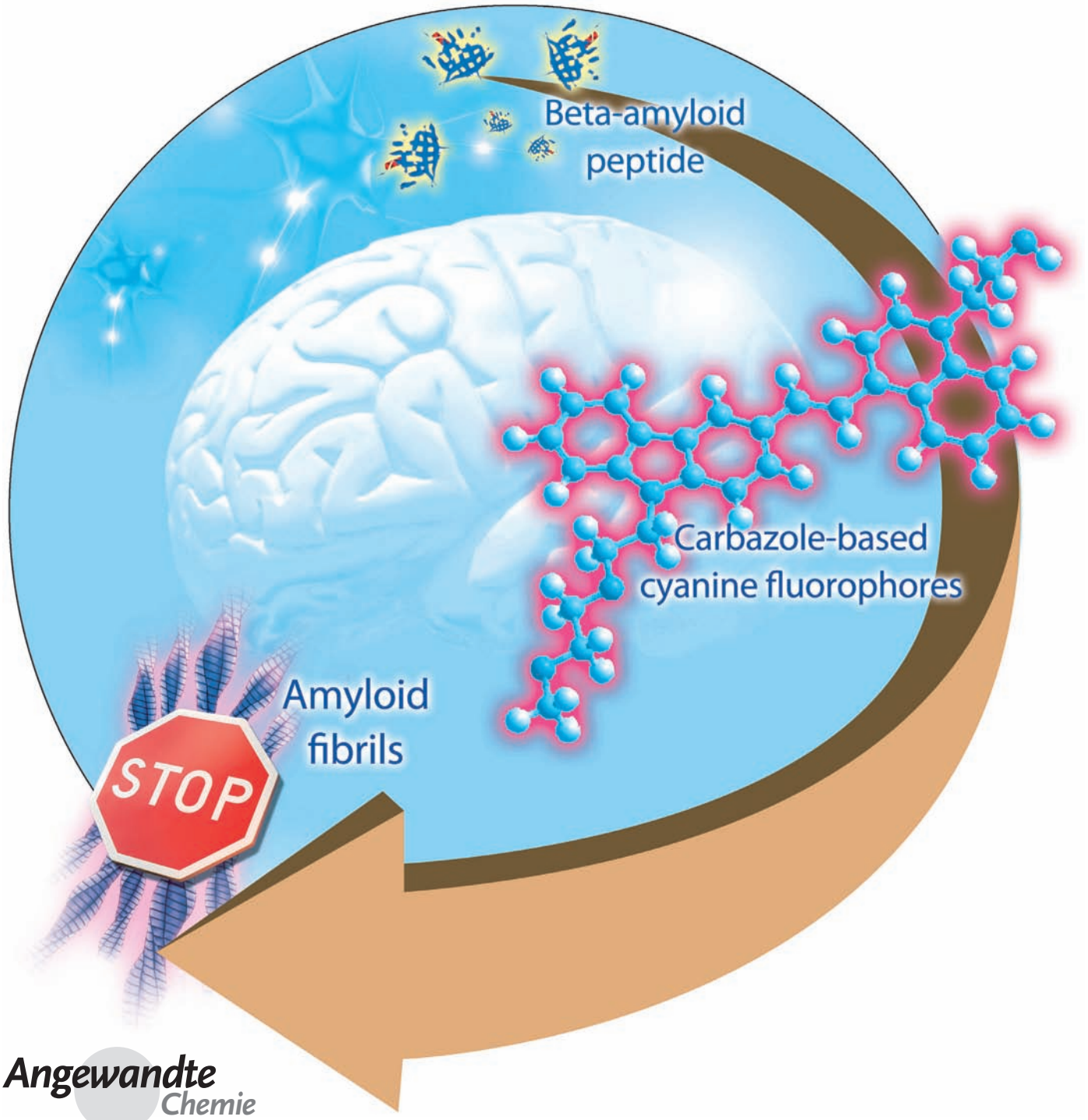

Alzheimer's disease (AD) affects more than 24 million people worldwide, leading to dementia, cognitive impairment and memory loss.[1] It is commonly accepted that beta-amyloid (Aβ) peptides of 40 and 42 residues formed from the cleavage of amyloid precursor protein play a key role in AD pathogenesis where the aggregation of monomeric Aβ peptides to insoluble plaque-associated amyloid fibrils via soluble oligomeric intermediates would induce a cascade of events that eventually lead to the death of neuronal cells.[2] The fibrillogenesis of Aβ is a two-phase process, involving nucleation and elongation phases, during which the Aβ peptides undergo conformational transition from predominantly unstructured form to a β-sheet-rich structure which stacks along the long axis of the fibrils through end-to-end annealing and the lateral association mechanism proposed by Walsh and co-workers.[3] Although a consensus mechanism to explain the pathogenic oligomeric assembly has yet to emerge, the development of a brain-penetrating agent that interferes with the aggregation of the Aβ peptides, thus inhibiting the formation of the neurotoxic oligomers and fibrils, is an attractive primary approach to the treatment of AD. Over the years, there have been numerous efforts to develop effective fibril inhibitors and β-sheet breakers that can prevent the aggregation of Aβ monomers into oligomeric and fibrillar conformations.[4] For instance, scyllo cyclohexanehexol has been developed as an Aβ-aggregation inhibitor and is currently under phase II clinical trial.[4b] Polyphenols and antioxidants have also been reported to inhibit Aβ fibrillogenesis and some are currently under clinical trials.[5]

Polymeric nanoparticles of various sizes and hydrophobicities have been used to adsorb the Aβ peptide onto the particle surface to control its fibrillogenesis kinetics.[6] Our previous work has demonstrated that ligand-functionalized quantum dots can quench both the nucleation and elongation of the $A\beta_{(1-40)}$ peptide by blocking active sites on the seed fibrils or monomers.[7] In addition to nanomaterials, transition-metal complexes, such as platinum(II),[8] binuclear ruthenium(II) platinum(II),[9] iridium(III) and rhodium(III) solvato[10] complexes have been utilized as potent inhibitors of Aβ aggregation by the formation of coordinative bond with amino acid residues of the peptides. To be clinically useful, these inhibitors or β-breakers must also have blood–brain barrier (BBB) permeability, low neurotoxicity, and high in vivo stability. However, these crucial properties have yet to be demonstrated in these inhibitors or β-breakers.

Recently, carbazole-based cyanine fluorophores have been shown to be a highly sensitive fluorescent light-up probe for double-stranded DNA and two-photon absorption dyes for two-photon excited bioimaging.[11] More recently, the mono-cyanine fluorophores have been found to bind to the Aβ peptide as well, concomitant with strong fluorescence enhancement (> 80 fold). This observation has provided us with a lead structure to develop novel functional molecules for a direct imaging of the dynamics of Aβ fibrillogenesis and, more importantly, for inhibiting the aggregation of Aβ peptides. Herein, a structure–activity investigation of a novel series of carbazole-based cyanine fluorophores that exhibit strong fluorescence enhancement upon binding with Aβ peptides and fibrils is reported. Using variously functionalized pyridinium or quinolinium accepting moieties, the functional properties, which include photophysical, Aβ-binding, cytotoxic, and BBB permeability properties, of these cyanine dyes can be modified and fine-tuned. One of these fluorophores, namely, SLOH (see Figure 1), is shown to inhibit the aggregation of Aβ peptides and oligomers, thus preventing the fibril growth. More importantly, this dye is non-toxic to the neuronal cells and exhibits a protective effect against the neurotoxic activities of the Aβ oligomers and fibrils. Its ability to penetrate the blood-brain barrier demonstrated its potential as a neuroprotective and/or therapeutic agent for Alzheimer's disease.

Figure 1 shows the molecular structures of carbazole-based cyanine fluorophores. By adapting the convergent approach established previously,[11] the Knoevenagel reaction of carbazolyl-3-aldehyde and the corresponding 4-alkylpyridinium or 4-alkyl-quinoliniumhalide was used as the key step to synthesize these carbazole-based monocyanines (see Supporting Information, Figure S1). All these cyanines were fully characterized by ^1H and ^{13}C NMR spectroscopy, mass spectrometry, and elemental analysis and the data obtained are in good agreement with the proposed structures.

These carbazole-based cyanines, which were highly soluble in aqueous solution, showed a broad and featureless absorption band peaked (λ_{max}^{abs}) at around 417–462 nm in phosphate buffer solution (Supporting Information, Figure S2). Upon excitation at their λ_{max}^{abs}, these compounds

[*] W. Yang,[+] Y. Wong,[+] Prof. D. W. J. Kwong, Prof. H.-W. Li, Prof. M. S. Wong
Department of Chemistry, Hong Kong Baptist University
Kowloon Tong, Hong Kong (P. R. China)
E-mail: hwli@hkbu.edu.hk
mswong@hkbu.edu.hk
Dr. O. T. W. Ng,[+] Prof. K. K. L. Yung
Department of Biology, Hong Kong Baptist University
Kowloon Tong, Hong Kong (P. R. China)
E-mail: kklyung@hkbu.edu.hk
Dr. L.-P. Bai, Prof. Z.-H. Jiang
School of Chinese Medicine, Hong Kong Baptist University
Kowloon Tong, Hong Kong (P. R. China)
Prof. Y. Ke
School of Biomedical Sciences, The Chinese University of Hong Kong
Shatin, Hong Kong (P. R. China)
[+] These authors contributed equally to this work.

[**] This work was financially supported by the Research Grant Council of the Hong Kong Special Administrative Region, P. R. China (HKBU201208 for H.W.L.; HKBU262107 and HKBU262210 for K.K.L.Y.; HKBU202408 for M.S.W.; and, HKBU2607/09M for Z.H.J.). K.K.L.Y. also thanks the Hong Kong Baptist University Research Committee (RC/AOE/08-09/02). We thank Mr. Chun-Tak Lau at Chemistry Department, Hong Kong University of Science and Technology for assistance with CD measurements. The FEI-Technai G2 TEM used in this work was supported by the Centre for Surface Analysis and Research (CSAR) with funding from the Special Equipment Grant from the University Grant Committee of the Hong Kong Special Administrative Region, China (SEG_HKBU06).

Supporting information for this article is available on the WWW under http://dx.doi.org/10.1002/anie.201104150.

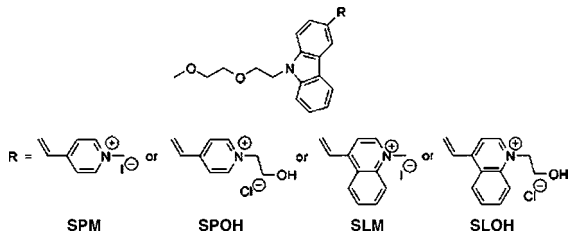

Figure 1. The molecular structure of carbazole-based cyanine fluorophores.

Table 1: Fluorescence enhancement and binding constant of carbazole-based cyanine dyes to Aβ.

	SPM	SPOH	SLM	SLOH
$F_{peptide}/F_{dye}$[a]	1.5	3.3	3.2	6.3
F_{fibril}/F_{dye}[b]	4.2	10.5	23.5	81.5
K_d[c] [μM]	194	459	49	92

[a] Fluorescence enhancement ratio measured at 100 equivalents of $A\beta_{(1-40)}$ peptide content. [b] Fluorescence enhancement ratio measured at 100 equivalents of $A\beta_{(1-40)}$ fibril content. [c] Dissociation constant to Aβ fibrils determined by nonlinear curve fitting, K_d (ThT) = 101 mM under the same measurement conditions.

exhibited a very weak emission at 596–677 nm, with fluorescence quantum yields (Φ_F) ranging from 0.001–0.05 (Supporting Information, Table S1). When these carbazole-based cyanines were titrated with the $A\beta_{(1-40)}$ peptide in phosphate buffer, a strong and progressive increase (up to 82-fold) in fluorescence intensity, concomitant with substantial blue shifts ($\Delta\lambda = 14$–22 nm) of the emission maxima, was seen. These spectral changes are indicative of an association of these fluorophores with $A\beta_{(1-40)}$ peptide (Supporting Information, Figure S3). The fluorescence enhancement was attributed to the large reduction in the non-radiative decay of the photo-excited cyanines due to a restricted rotation upon Aβ peptide binding. The binding interaction of the carbazole-based cyanines with Aβ peptide was corroborated by the observation of various adducts in the electrospray ionization time-of-flight mass spectrometry (ESI-TOF-MS) of these solution mixtures. The mass spectra obtained from the mixtures of $A\beta_{(1-40)}$ peptide and the carbazole-based cyanines are shown in Figure S4 in the Supporting Information. Various adducts from 1:1 to 1:4 binding stoichiometries formed between the $A\beta_{(1-40)}$ peptide and the carbazole-based cyanines were observed and identified from these spectra. The results from the binding studies (Supporting Information, Table S2), demonstrated that SLOH shows the highest binding affinity with $A\beta_{(1-40)}$ peptide among all the carbazole-based cyanines.[12]

More importantly, the fluorescence enhancement (F) was much stronger for Aβ fibril than for Aβ peptide (e.g., $F_{fibril}/F_{SLOH} = 81.5$ versus $F_{peptide}/F_{SLOH} = 6.3$ in the presence of 100 equivalents of $A\beta_{(1-40)}$ peptide, with or without seeded Aβ fibril, Figure 2e, Table 1). To ascertain the binding affinities of these fluorophores towards $A\beta_{(1-40)}$ fibril, the dissociation constants (K_d) were determined from the fluorescence titration curves by nonlinear curve fitting (Table 1).[13] The binding affinities of the quinolinium-based fluorophores (K_d for SLM and SLOH = 49 and 92 μM, respectively) for Aβ fibril were 2- to 9-fold higher than those of the pyridinium-based fluorophores (K_d for SPM and SPOH = 194 and 459 μM, respectively), suggesting the importance of the π–π stacking interaction for such an association. Furthermore, the K_d of these quinolinium-based fluorophores was comparable to that of the conventionally used Aβ fibril-labeling dye, thioflavin T (ThT, $K_d = 101$ μM). These observations suggest that these fluorophores can potentially be used as fluorescent labeling and imaging dyes for $A\beta_{(1-40)}$ peptide, fibril and plaque. In addition, comparing to ThT, these fluorophores offer wider wavelength range for the excitation and imaging of $A\beta_{(1-40)}$ peptide and its aggregated forms. Figure 2a–d shows the direct imaging of Aβ peptide and its fibril using these four fluorophores. Their strong fluorescence enhancement (with good signal-to-noise ratio) upon binding with the Aβ fibril allowed us to monitor the growth of single fibrils.

The effects of these carbazole-based cyanines on $A\beta_{(1-40)}$ fibrillogenesis were investigated by monitoring the non-seeded and seed-mediated growth of $A\beta_{(1-40)}$. Taking advantage of the native fluorescence properties and the difference in fluorescence enhancement of the carbazole-based dye upon binding to monomeric and aggregated Aβ peptides, fibrillogenesis kinetics in the presence of SLM and SLOH were studied and compared with that from ThT assay (Figure 3a). In the non-seeded growth, typical sigmoidal growth curve was seen in the ThT assay, but fibrillogenesis was retarded by SLM and completely inhibited by SLOH. Similar results were also obtained in the seed-mediated growth experiment (Supporting Information, Figure S5).

Total internal reflection fluorescence microscopy (TIRFM) was also applied to estimate the population and sizes of aggregates/fibrils resulted from a 24 h incubation of the Aβ monomer with and without SLOH. No Aβ aggregates were found in the presence of SLOH, but in the absence of SLOH, long $A\beta_{(1-40)}$ fibrils were observed (Supporting Information, Figure S6), apparently resulting from self-aggregation of the Aβ monomers. In the seed-mediated growth, SLOH was consistently found to show a complete inhibitory effect on the elongation of the Aβ fibril seeds while other cyanines, namely, SPM, SPOH, and SLM, displayed weaker inhibitory effect under identical experimental conditions. Both TIFRM and transmission electron microscopic (TEM) images (Figure 3c) showed only the preformed seed fibrils, with no elongated fibrils, were found in the incubation mixture containing the seed fibrils, Aβ monomers and SLOH. Interestingly, a partial structural analogue of SLOH, namely 1-(2-hydroxyethyl)-4-methylquinolinium chloride, showed no inhibitory effect on Aβ fibril growth as monitored by the TIRFM experiment. This further shows that the unique structural entity of SLOH is essential for its potent inhibitory effect on SLOH on Aβ fibrillogenesis. The inhibitory effect of SLOH on Aβ fibrillogenesis was further evaluated at different time points during a one hour-incubation. SLOH was added at different time points (0, 10, 20, 30, 40, and 60 min) to the incubation mixtures containing the Aβ monomers and its fibril seeds. The average lengths of the resulting fibrils were

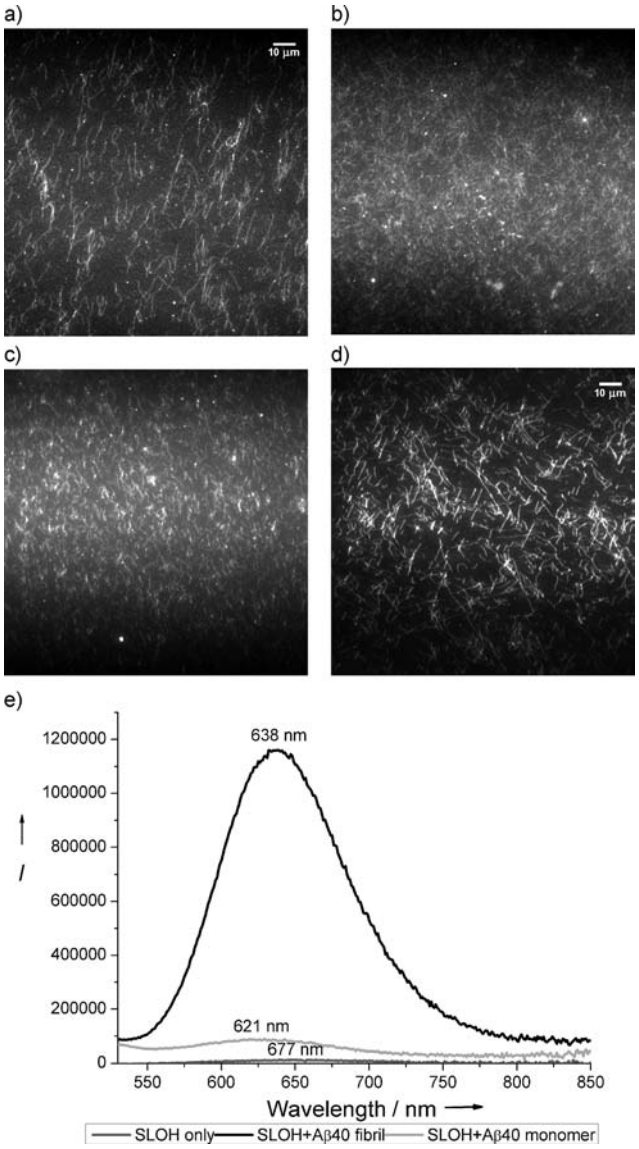

Figure 2. TIRFM images of $A\beta_{(1-40)}$ fibrils labeled with a) SPM; and b) SPOH excited at 445 nm; c) SLM and d) SLOH excited at 488 nm. e) Fluorescence spectra of 1 μM carbazole-based fluorophores SLOH (dark gray), 1 μM SLOH with 100 equivalent of $A\beta_{(1-40)}$ peptide (light gray), and 1 μM SLOH with 100 equivalent of $A\beta_{(1-40)}$ fibrils (black) in phosphate buffer of pH 7.4. Scale bars 10 μm.

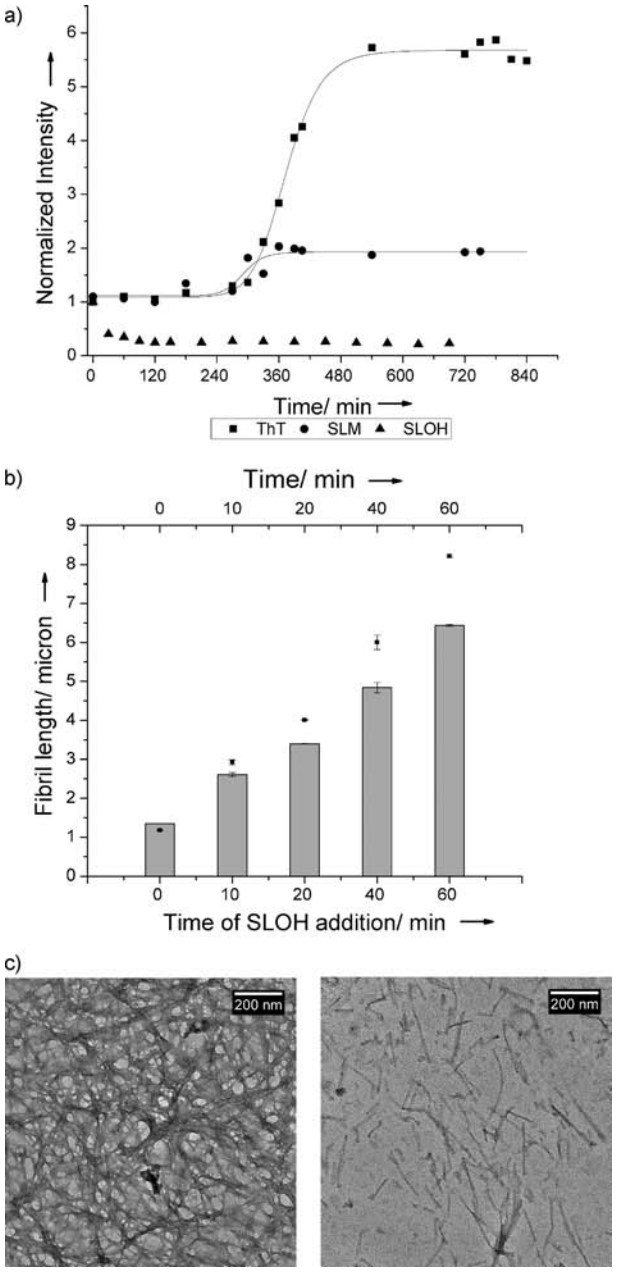

Figure 3. Inhibition of $A\beta_{(1-40)}$-fibril growth by SLOH. a) ThT, SLM, and SLOH fluorescence binding assays for 50 μM $A\beta_{(1-40)}$ fibrillation. b) Average length of 1 h incubated $A\beta_{(1-40)}$-fibril measured from TIRFM images after 1 h seed-mediated incubation of Aβ monomer with SLOH (50 μM) added at different times within an one hour-incubation (bottom axis, bars). In the control experiment, the length of $A\beta_{(1-40)}$ fibrils was measured at 0, 10, 20, 40, and 60 min without the addition of SLOH (top axis, filled squares). c) TEM images of $A\beta_{(1-40)}$ fibril grown in the absence (left) and the presence (right) of SLOH after 1 h incubation at 37 °C by seed-mediated growth.

measured by TIRFM and shown in Figure 3b, together with the results from the corresponding control experiments (i.e., without addition of SLOH) conducted in parallel under identical conditions. The inhibitory effect on Aβ fibril growth appeared to be almost instantaneous after the addition of SLOH. These results clearly demonstrate the inhibitory effect of SLOH on both the $A\beta_{(1-40)}$ nucleation and elongation processes.

To investigate the mechanism of the inhibitory action of SLOH, we examined its effects on Aβ peptide and fibril in an aqueous solution by the circular dichroism (CD). It is generally accepted that the Aβ aggregate results from a conformational change of the Aβ peptide from its non-amyloidogenic random coil conformer to the amyloidogenic conformer with extensive β-sheet character, which then oligomerizes to the neurotoxic intermediates and amyloid plaques.[14] The CD spectra of were recorded of Aβ peptide and fibril in the presence and the absence of SLOH and another carbazole-based cyanine, SLM, which showed no Aβ fibrillogenesis inhibitory effect (Supporting Information, Fig-

ure S7). In the absence of the carbazole-based cyanines, the monomeric Aβ peptide gave a weak negative CD signal at 220 nm, characteristic wavelength of β-sheet-like character. This notion is corroborated by the stronger negative CD signal at 220 nm observed in the seeded Aβ fibril showing more extensive β-sheet character. However, upon addition of SLOH, the negative CD signals of both the monomeric and fibrillar Aβ peptide shifted from 220 nm to 230 nm, indicating that the relative population of β-sheet conformer was significantly diminished and a new conformation, perhaps an Aβ-SLOH adduct, resulted (Supporting Information, Figure S7a). This decrease in the β-sheet conformer population appeared almost immediately upon SLOH addition. In contrast, an addition of SLM produced no significant change to the CD profiles of both the monomeric and fibrillar Aβ peptide (Supporting Information, Figure S7b). Even though both SLOH and SLM have been shown to bind to both the Aβ peptide and fibril, albeit with a 2-fold difference in binding affinity towards Aβ fibril (Table 1), their ability to change the amyloidogenic conformer ($A\beta_{ac}$) was very distinct, indicating that their binding interactions (including their binding sites) with both the monomeric and fibrillar Aβ peptide must be distinct. This result also reinforces the notion of a close association between the β-sheet conformer of Aβ peptide and its propensity for fibrillogenesis.[10,14]

To ascertain the clinical application of the carbazole-based cyanines, the cytotoxicity of these compounds towards human neuroblastoma SH-SY5Y neuronal cells were evaluated. The cytotoxicity of different concentrations of the four carbazole-based molecules (10 nM, 1 μM, 10 μM, and 50 μM) upon exposure for 2, 6, and 24 h was determined using the MTT assay (Supporting Information, Figure S8). The result shows that no significant cytotoxicity (< 20 %) of SLOH was seen at concentrations of ≤ 1 μM from 2 to 24 h of exposure. Maximum cytotoxicity (ca. 35 %) was seen at 50 μM for 24 h exposure. Interestingly, the cytotoxicity of SLOH at concentrations less than or equal to 1 μM was quite similar for 2 and 6 h exposure. As for the other carbazole-based cyanines, SPM, SPOH, and SLM, their cytotoxicities (Supporting Information, Figure S8a-c) were not considered high (< 35 %) even at 50 μM and 24 h exposure, except for SLM. Thus, no potent cytotoxic effects were found with these carbazole-based cyanines towards the neuronal cell studied.

The effect of SLOH on the $A\beta_{(1-40)}$-induced cytotoxicity on the SH-SY5Y cells and mouse primary cortical cells were also investigated. In the absence of $A\beta_{(1-40)}$, SLOH non-specifically diffused into the cell while in the presence of added $A\beta_{(1-40)}$ peptides, SLOH shows its high selectivity toward $A\beta_{(1-40)}$. The selectivity was confirmed with antibody labeling (Supporting Information, Figure S9). The cytotoxicity of three different forms of $A\beta_{(1-40)}$ peptide: 1) $A\beta_{(1-40)}$ peptide monomer (M), 2) $A\beta_{(1-40)}$ peptide monomer with seeded fibril (MS), and 3) $A\beta_{(1-40)}$ fibril (F), were examined in the presence and the absence of SLOH (Figure 4). A relative cytotoxicity of less than one indicates a protective effect of SLOH against the cytotoxic action of the Aβ peptide towards the neuronal cell. A neuroprotective effect of SLOH is clearly seen in the cytotoxic activities induced by all three forms of $A\beta_{(1-40)}$ peptide and at [SLOH]/[Aβ] of 0.2, 1.0, and 5 for both

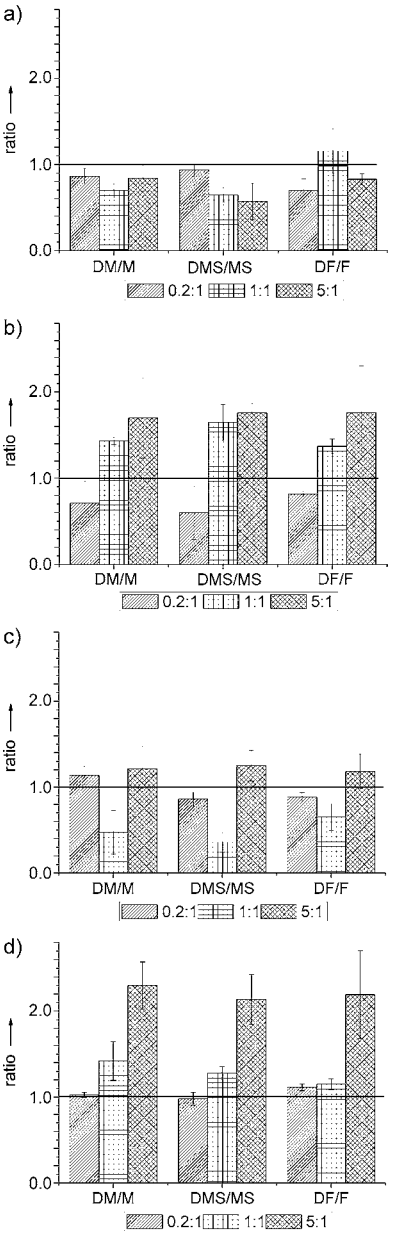

Figure 4. Neuroprotective effects of SLOH against various forms of $A\beta_{(1-40)}$ peptide-induced cytotoxicity towards a),b) human neuroblastoma SH-SY5Y cells and c),d) mouse primary cortical cells. The histograms show the relative cytotoxicity of 10 μM of $A\beta_{(1-40)}$ peptide monomer (M), $A\beta_{(1-40)}$ peptide with seeded fibril (MS), and fibrillar $A\beta_{(1-40)}$ peptide (F), in the presence of SLOH. Various forms of $A\beta_{(1-40)}$ peptide were incubated a),c) for 2 h, and b),d) for 24 h at [SLOH]:[Aβ] of 0.2:1, 1:1, and 5:1. The relative cytotoxicity was calculated from the cytotoxicity measured for different forms of Aβ peptide with SLOH relative to that without, that is, DM/M = (SLOH + M)/M; DMS/MS = (SLOH + MS)/MS; and DF/F = (SLOH + F)/F. D = SLOH.

SH-SY5Y cells and primary cells after 2 h of incubation (Figure 4 a,c). No significant neuroprotection for 6 h incubation was observed (Supporting Information, Figure S10). After 24 h of incubation, for SH-SY5Y cells, the relative cytotoxicity induced by all three forms of Aβ peptide in the presence of SLOH became higher than one, indicating an

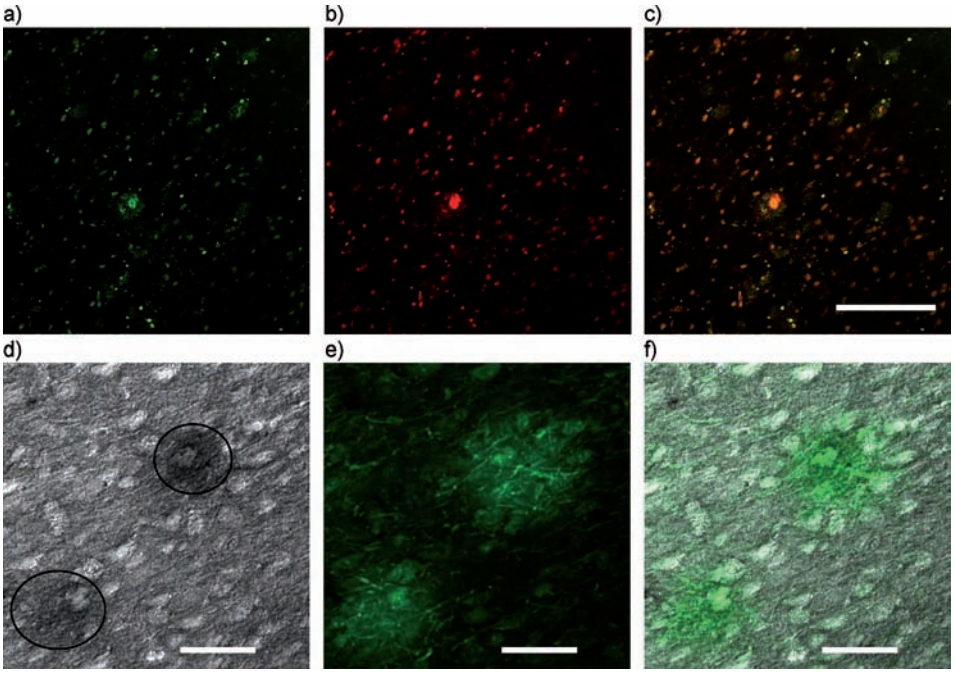

Figure 5. Fluorescence images of transgenic mice brain with tail vein injection of SLOH and co-stained with the Aβ labeling dye, ThT, or Aβ antibody with DAB stain. Fluorescence images corresponding to a) SLOH fluorescence captured at 550–630 nm under excitation at 488 nm; b) ThT fluorescence captured at 470–550 nm under excitation at 458 nm; and c) overlapped images of (a) and (b), scale bar 200 μm. The overlapped image reveals the colocalization of fluorescence signals of SLOH and ThT in cellular components. d) Differential interference contrast (DIC) image of DAB-stained brain slides of transgenic mice. e) Fluorescence image of same slide corresponding to SLOH fluorescence captured at 550–630 nm under excitation at 488 nm; and f) overlapped images of (d) and (e). The overlapped image reveals the colocalization of fluorescence signals of SLOH and Aβ antibody in cellular components. Scale bars 40 μm.

additional cytotoxic effect due to SLOH (Figure 4b,d). It was found that primary cortical cells were more sensitive to toxicity of both Aβ and SLOH. However, it is highly significant to observe that SLOH exerted its neuroprotective effect, for SH-SY5Y cells but not primary cortical cells, when present at a sub-stoichiometric (binding) concentration ratio of 0.2 even after long period (24 h) of incubation. This result indicated that SLOH was neuroprotective when administered at a low enough dosage and thus showing therapeutic potential.

To further explore the potential clinical applications of SLOH, its abilities to pass through the BBB of live animals and to target the Aβ plaque in transgenic mice was demonstrated. Tail vein injection and brain immersion with SLOH were performed in non-transgenic and transgenic mice of 6-month of age, which have already shown human Aβ plaque developed in the brain. Brain slices were obtained from wild-type (non-transgenic) mice and transgenic mice 30 min after tail-vein injection of SLOH. For the control experiment, brain slices of mice without SLOH treatment were directly immersed into SLOH solution for comparison. Fluorescence images of the brain slices were captured with laser scanning confocal microscopy (Supporting Information, Figure S11a–c). Fluorescence images obtained from these three experiments showed clearly different patterns. The control brain slice showed homogeneous native fluorescence. However, with tail vein injection of SLOH, a different fluorescence pattern was observed as SLOH labeled some cellular structures. The brain slices of the transgenic mice showed large fluorescent clusters that are not seen in those of wild-type mice. It was expected that these clusters were the Aβ plaque. A maximum fluorescence emission at around 600 nm was found from both the transgenic and wide-type brain slices. The confocal lambda scans of these signals matched well with the emission spectrum of SLOH obtained under cell-based conditions. These results indicated that SLOH was able to pass through the BBB. To further identify the fluorescent clusters observed, we co-stained the brain slices of SLOH-injected mice with the Aβ plaque-labeling ThT dye. The fluorescence images of the SLOH emission (Figure 5a) and ThT emission (Figure 5b) were merged to give Figure 5c. The overlapping images revealed the co-localization of fluorescence signals of SLOH and ThT in cellular components, which also indicated that fluorescence signals detected in cellular components corresponded to the Aβ aggregates in the transgenic mice (Figure 5c). In another independent experiment, an Aβ antibody was used to identify the Aβ plaques in transgenic mice's brain. Figure 5d–f shows the selectivity of SLOH towards Aβ plaques as confirmed with Aβ antibody. These results further affirm that SLOH can pass through the BBB to target the Aβ plaque over other cellular components in the mouse model.

In summary, we have demonstrated that carbazole-based cyanine fluorophores bind selectively to $A\beta_{(1-40)}$ peptides, aggregates, and plaques resulting in strong fluorescence enhancement, making a direct imaging and labeling of these important biological targets possible. The effects of these molecules on Aβ aggregation/fibrillogenesis were also studied. These carbazole-based fluorophores were shown to be generally non-toxic to the neuronal cells. More importantly, one of these fluorophores, SLOH, was shown to exert a strong inhibitory effect on $A\beta_{(1-40)}$ fibrillogenesis, which correlated with a decrease in the β-sheet-like conformer population detected by circular dichroism. A neuroprotective effect of SLOH against the $A\beta_{(1-40)}$-induced cytotoxicity towards the neuronal cells was also demonstrated. These results, together with the demonstrated abilities of SLOH to pass through the blood-brain barrier and targets the Aβ plaque, make it a

potential neuroprotective and therapeutic agent for Alzheimer's disease. This work opens up a new avenue to develop potent Aβ-aggregation inhibitors with BBB permeability.

Received: June 16, 2011
Revised: August 31, 2011
Published online: November 15, 2011

Keywords: Alzheimer's disease · beta-amyloid peptide · fluorophores · inhibitors

[1] R. Jakob-Roetne, H. Jacobsen, *Angew. Chem.* **2009**, *121*, 3074; *Angew. Chem. Int. Ed.* **2009**, *48*, 3030.
[2] D. J. Selkoe, *J. Neuropathol. Exp. Neurol.* **1994**, *53*, 438.
[3] D. M. Walsh, A. Lomakin, G. B. Benedek, M. M. Condron, D. B. Teplow, *J. Biol. Chem.* **1997**, *272*, 22364.
[4] a) M. G. Chini, M. Scrima, A. M. D'Ursi, G. Bifulco, *J. Pept. Sci.* **2009**, *15*, 229; b) J. McLaurin, M. E. Kierstead, M. E. Brown, C. A. Hawkes, M. H. L. Lambermon, A. L. Phinney, A. A. Darabie, J. E. Cousins, J. E. French, M. F. Lan, F. S. Chen, S. S. N. Wong, H. T. J. Mount, P. E. Fraser, D. Westaway, P. St. George-Hyslop, *Nat. Med.* **2006**, *12*, 801; c) T. H. Vu, T. Shimanouchi, N. Shimauchi, H. Yagi, H. Umakoshi, Y. Goto, R. Kuboi, *J. Biosci. Bioeng.* **2010**, *109*, 629.
[5] Y. T. Choi, C. H. Jung, S. R. Lee, J. H. Bae, W. K. Baek, M. H. Suh, J. Park, C. W. Park, S. I. Suh, *Life Sci.* **2001**, *70*, 603.
[6] C. Cabaleiro-Lago, F. Quinlan-Pluck, I. Lynch, S. Lindman, A. M. Minogue, E. Thulin, D. M. Walsh, K. A. Dawson, S. Linse, *J. Am. Chem. Soc.* **2008**, *130*, 15437.
[7] L. H. Xiao, D. Zhao, W. H. Chan, M. M. F. Choi, H. W. Li, *Biomaterials* **2010**, *31*, 91.
[8] K. J. Barnham, V. B. Kenche, G. D. Ciccotosto, D. P. Smith, D. J. Tew, X. Liu, K. Perez, G. A. Cranston, T. J. Johanssen, I. Volitakis, A. I. Bush, C. L. Masters, A. R. White, J. P. Smith, R. A. Cherny, R. Cappai, *Proc. Natl. Acad. Sci. USA* **2008**, *105*, 6813.
[9] A. Kumar, L. Moody, J. F. Olaivar, N. A. Lewis, R. L. Khade, A. A. Holder, Y. Zhang, V. Rangachari, *ACS Chem. Neurosci.* **2010**, *1*, 691.
[10] B. Y.-W. Man, H.-M. Chan, C.-H. Leung, D. S.-H. Chan, L.-P. Bai, Z.-H. Jiang, H.-W. Li, D.-L. Ma, *Chem. Sci.* **2011**, *2*, 917.
[11] X. J. Feng, P. L. Wu, F. Bolze, H. W. C. Leung, K. F. Li, N. K. Mak, D. W. J. Kwong, J. F. Nicoud, K. W. Cheah, M. S. Wong, *Org. Lett.* **2010**, *12*, 2194.
[12] E. Martineau, J. M. de Guzman, L. Rodionova, X. Q. Kong, P. M. Mayer, A. M. Aman, *J. Am. Soc. Mass Spectrom.* **2010**, *21*, 1506.
[13] Q. Li, J. K. Min, Y. H. Ahn, J. H. Namm, E. M. Kim, R. Lui, H. Y. Kim, Y. Ji, H. Z. Wu, T. Wisniewski, Y. T. Chang, *ChemBioChem* **2007**, *8*, 1679.
[14] D. J. Tew, S. P. Bottomley, D. P. Smith, G. D. Ciccotosto, J. Babon, M. G. Hinds, C. L. Masters, R. Cappai, K. J. Barnham, *Biophys. J.* **2008**, *94*, 2752.

